Factorization and nonfactorization in *B* decays

F. M. Al-Shamali and A. N. Kamal
Theoretical Physics Institute and Department of Physics, University of Alberta, Edmonton, Alberta, Canada T6G 2J1
(Received 9 June 1999; published 5 November 1999)

Using NLL values for Wilson coefficients and including the contributions from penguin diagrams, we estimate the amount of nonfactorization in two-body hadronic *B* decays. Also, we investigate the model dependence of the nonfactorization parameters by performing the calculation using different models for the form factors. The results support the universality of nonfactorizable contributions in both Cabibbo-favored and Cabibbo-suppressed *B* decays. [S0556-2821(99)06623-0]

PACS number(s): 13.25.Hw, 14.40.Nd

I. INTRODUCTION

The decay rates (and, in few cases, polarization) of a large number of hadronic channels have been experimentally measured to sufficient accuracy. However, as yet there is no reliable theoretical method to derive the corresponding amplitudes starting from the basic principles of the standard model. This is due to our inability to quantify the participation of strong interactions in such processes. The powerful theoretical tools of perturbation theory which are used in purely electroweak interactions are not very useful in situations involving strong interactions. Nonperturbative techniques, such as lattice calculations and QCD sum rules, are still under development. However, the asymptotic freedom property of QCD allows us to separate the gluon contribution, in a given process, into that due to high energy (hard) gluons and that due to low energy (soft) gluons. The former contribution is relatively easy to compute using perturbation techniques and renormalization group equations. In fact, an impressive amount of work in this regard has been done [1–6], where hard gluon effects were parametrized through Wilson coefficients which have been calculated up to next-to-leading logarithmic (NLL) order. It is the soft gluon contribution which is difficult to handle and constitutes the main source of uncertainty in hadronic weak decays.

In general, the effective Hamiltonian in hadronic decays of *B* mesons takes the form $H_{\rm eff}\sim\Sigma_i C_i Q_i$ where *C*'s are the Wilson coefficients that contain the hard gluon (or short distance) effects and *Q*'s are four-quark operators that are products of two Dirac currents. In calculating the decay amplitudes for two-body hadronic decays we then encounter matrix elements of the form $\langle f_1 f_2|Q|i\rangle$, where i is the initial-state particle, and f_1 and f_2 are the final-state particles. In phenomenological calculations, the factorization assumption (i.e., the matrix element of a current $\times$ current operator is equal to the product of the matrix elements of the current operators) is commonly invoked. As a result, the decay amplitudes for processes with external *W* emission (class I processes) are proportional to [7] $a_1=C_1+C_2/N_c$ where N_c is the number of colors. Similarly, the decay amplitudes for processes with internal *W* emission (class II processes) are proportional to $a_2=C_2+C_1/N_c$.

The effect of nonfactorization in *B* decays has been studied by several authors in the past using different parametrization methods. For example, some authors [8–10] treated N_c as a free parameter whose effective value is used to indicate the amount of nonfactorization in a decay process. Others [11–14] have used ($N_c=3$) and parametrized the the nonfactorizable matrix elements in the decay amplitude. In this paper, we continue to use the same parametrization adopted in the previous work [15]; i.e., the nonfactorized effects caused by the color singlet and color octet currents are parametrized in terms of the two parameters ε_1 and ε_8, respectively. These parameters are introduced into the decay amplitude through the replacements

$$a_1\to a_1^{\rm eff}=a_1\left(1+\varepsilon_1+\frac{C_2}{a_1}\varepsilon_8\right),$$

$$a_2\to a_2^{\rm eff}=a_2\left(1+\varepsilon_1+\frac{C_1}{a_2}\varepsilon_8\right). \tag{1}$$

One of the issues that arises when parametrizing nonfactorizable contributions is how to handle processes with two vector mesons in the final state. This is because it is not clear whether or not the three Lorentz scalar structures of the decay amplitude should receive the same contribution from the nonfactorizable terms; i.e., does nonfactorization lead verily to an overall factor? This issue was discussed in Refs. [12,11]. In Ref. [16] we tackled this issue in some detail for the process $B\to J/\psi K^*$. Using a full amplitude measurement [17] by CLEO, the amount of nonfactorizable contribution to each of the three Lorentz-scalar structures was calculated in five different models for the form factors. The results allowed an explanation of the experimental data using equal amount of nonfactorization in each part of the Lorentz amplitude, implying that an overall nonfactorization factor was adequate.

Assuming universality (process independence) of the nonfactorization parameters in *B* decays, we estimated their values in Ref. [15] using a more definitive calculation. However, for the Wilson coefficients we used the values calculated up to leading logarithmic (LL) order and neglected all contributions from the penguin diagrams. Also, all the calculations were done using only one model for the form factors [Bauer-Stech-Wirbel (BSW) II model]. The results supported the proposition of the universality of the nonfactorization parameters in Cabibbo-favored *B* decays. However, a number of questions were also raised. First, how will the results change if we use the Wilson coefficients calcu-

lated up to NLL order? Second, how do we parametrize the nonfactorization generated by penguin diagrams and how important they are? Third, how much model dependence is there in the estimated nonfactorization parameters? Finally, can we extend the proposed universality of the nonfactorization parameters to include Cabibbo-suppressed B decays? These are the questions we try to address in this paper.

The paper is arranged as follows: In Sec. II we present the Wilson coefficients and Cabibbo-Kobayashi-Maskawa (CKM) matrix elements used in the calculations. In Sec. III we calculate the effects of penguin diagrams and NLL Wilson coefficients on the predictions of naive factorization. In Sec. IV the nonfactorization parameters are estimated in five models for the form factors. In Sec. V we show branching ratio predictions of several sets of Cabibbo-favored and Cabibbo-suppressed B decays. The last section is a discussion of the results and a conclusion.

II. WILSON COEFFICIENTS IN NLL ORDER

In the absence of strong interactions, the effective Hamiltonian for the process $b\to c\bar{c}s$, is given by

$$\mathcal{H}_{\rm eff}=\frac{G_F}{\sqrt{2}}V_{cb}V_{cs}^*(\bar{c}_ib_i)_L(\bar{s}_jc_j)_L. \tag{2}$$

When QCD effects are included, the contribution of the penguin diagrams should be considered beside the current $\times$ current diagrams. As a result, the effective Hamiltonian generalizes to [8,10]

$$\mathcal{H}_{\rm eff}=\frac{G_F}{\sqrt{2}}\Bigg[V_{ub}V_{us}^*(C_1Q_1^u+C_2Q_2^u)+V_{cb}V_{cs}^*(C_1Q_1^c+C_2Q_2^c) +(V_{ub}V_{us}^*+V_{cb}V_{cs}^*)\sum_{i=3}^{6}C_iQ_i\Bigg], \tag{3}$$

where

$$\begin{aligned}
Q_1^q&=(\bar{q}_ib_i)_L(\bar{s}_jq_j)_L,\\
Q_2^q&=(\bar{q}_ib_j)_L(\bar{s}_jq_i)_L,\quad q=u,c,\\
Q_3&=(\bar{s}_ib_i)_L\sum_q(\bar{q}_jq_j)_L,\\
Q_4&=(\bar{s}_ib_j)_L\sum_q(\bar{q}_jq_i)_L,\\
Q_5&=(\bar{s}_ib_i)_L\sum_q(\bar{q}_jq_j)_R,\\
Q_6&=(\bar{s}_ib_j)_L\sum_q(\bar{q}_jq_i)_R.
\end{aligned} \tag{4}$$

The subscripts L and R represent left-handed and right-handed currents, respectively. Even though the local operators Q_1^u and Q_2^u do contribute to processes of the type $b\to c\bar{c}s$ through tree diagrams, they do not contribute through penguin diagrams.

In NLL calculations, the Wilson coefficients turn out to be regularization scheme dependent. However, if the matrix elements $\langle Q_i(\mu)\rangle$ are evaluated at the same scheme as the Wilson coefficients $C_i(\mu)$, the scheme dependence cancels out. From Eq. (3), we see that the decay amplitude in the effective theory has the form

$$\begin{aligned}
\mathcal{A}_{\rm eff}&\propto C_i(\mu)\langle Q_i(\mu)\rangle\\
&\propto C_i(\mu)g_{ij}(\mu)\langle Q_j\rangle^{\rm tree}\\
&\propto C_i^{\rm eff}\langle Q_i\rangle^{\rm tree}.
\end{aligned} \tag{5}$$

At the quark level, the scale and scheme dependences of $\langle Q_i(\mu)\rangle$, which is carried by $g(\mu)$, cancel the scale and scheme dependences of the Wilson coefficients [8,10,18,19]. So both $C_i^{\rm eff}$ and $\langle Q_i\rangle^{\rm tree}$ are scale and scheme independent. From above, we can write the decay amplitude as

$$\langle\mathcal{H}_{\rm eff}\rangle=\frac{G_F}{\sqrt{2}}\Bigg[V_{cb}V_{cs}^*(C_1^{\rm eff}\langle Q_1^c\rangle^{\rm tree}+C_2^{\rm eff}\langle Q_2^c\rangle^{\rm tree}) +\sum_{i=3}^{6}(V_{ub}V_{us}^*C_i^{u\ {\rm eff}}+V_{cb}V_{cs}^*C_i^{c\ {\rm eff}})\langle Q_i\rangle^{\rm tree}\Bigg], \tag{6}$$

where the penguin contributions from $\langle Q_{i=1,2}^u\rangle$ and $\langle Q_{i=1,2}^c\rangle$ are included in $C_{i=3,\ldots,6}^{u\ {\rm eff}}$ and $C_{i=3,\ldots,6}^{c\ {\rm eff}}$, respectively. The details of calculating $C_i^{\rm eff}$ can be found in Ref. [8].

The calculation of the penguin-driven amplitudes in the factorization assumption involves additional assumptions, an effective value of k^2, for example. In a complete calculation [20] k^2 would not be a variable; it would be integrated over the wave functions of the hadrons with its own uncertainties. In the absence of a complete knowledge of the hadronic wave functions, the choice is either to select k^2 judiciously or to admit new unknowns through the hadronic wave functions. In penguin calculations, one generally opts for the first alternative and chooses k^2 in the range $m_b^2/4\leqslant k^2\leqslant m_b^2/2$. In the calculations presented here we have chosen $k^2=m_b^2/2$.

In Table I, we show the values of the Wilson coefficients in LL and NLL order (working in the naive dimensional regularization scheme) evaluated at the scale $\mu=4.6$ GeV. Also, we show the values of the effective Wilson coefficients $C_i^{\rm eff}$. For $C_3^{\rm eff}$–$C_6^{\rm eff}$, which include the contributions from the QCD penguin diagrams, we list two sets of values, corresponding to the u and c loop flavors. For quark masses, we used the the following running values at the b-quark mass scale [21]: $m_u=3.17$ MeV, $m_d=6.37$ MeV, $m_s=0.127$ GeV, $m_c=0.949$ GeV, $m_b=4.34$ GeV, and $m_t=170$ GeV. As for the CKM matrix elements, we used [22] $V_{ud}=0.976$, $V_{us}=0.221$, $V_{ub}=0.00316\,e^{-1.43i}$, $V_{cd}=-0.221$, $V_{cs}=0.976$, and $V_{cb}=0.0394$.

TABLE I. The second and third columns show the Wilson coefficients in LL and NLL order, respectively, evaluated at the scale $\mu=4.6$ GeV, and for $\Lambda^{5}_{\overline{\rm MS}}=219$ MeV. The last column shows the effective Wilson coefficients in NLL order, evaluated using the running quark masses. For $C_3^{\rm eff}$–$C_6^{\rm eff}$, two values are listed, corresponding to the two loop flavors in the penguin diagram.

	LL	NLL	Effective
C_1	1.127	1.075	1.143
C_2	−0.286	−0.178	−0.322
			$q=u(c)$
C_3	0.013	0.012	$0.0184+0.0048i\,(0.0197+0.0044i)$
C_4	−0.029	−0.033	$-0.0407-0.0145i\,(-0.0453-0.0132i)$
C_5	0.008	0.009	$0.0130+0.0045i\,(0.0145+0.0044i)$
C_6	−0.037	−0.039	$-0.0522-0.0145i\,(-0.0568-0.0132i)$
a_1	1.032	1.016	1.036
a_2	0.090	0.180	0.059
C_2/a_1	−0.277	−0.175	−0.311
C_1/a_2	12.54	5.96	19.37

III. DECAY RATES IN NAIVE FACTORIZATION

In decays of type $b\to c\bar{u}d$ only tree diagrams contribute to the decay amplitudes. In processes of class I (for example, $\bar{B}^0\to D^+\pi^-$) the factorizable part of the amplitude is proportional to a_1. As can bee seen from Table I, the value of this parameter in LL order ($a_1^{\rm LL}=1.032$) is almost the same as that in NLL order ($a_1^{\rm NLL}=1.036$). Since the decay rates are proportional to $|a_1|^2$, the above values for a_1 give a difference ($\Delta\mathcal{B}_{\rm fac}$) of less than 1% between the branching ratios calculated using the Wilson coefficients in LL order and the branching ratios calculated using the Wilson coefficients in NLL order (see Table II). In processes of class II (for example, $\bar{B}^0\to D^0\pi^0$), the factorizable part of the decay amplitude is proportional to a_2. This parameter takes the values ($a_2^{\rm LL}=0.090$) and ($a_2^{\rm NLL}=0.059$) in LL and NLL order, respectively. As a result, the predicted branching ratios (see Table II) in the naive factorization approximation drop by about 57% when working in NLL order. The decay amplitudes for class III processes (for example $B^-\to D^0\pi^-$) receive contributions from two tree diagrams, causing a dependence on both a_1 and a_2. Therefore, $\Delta\mathcal{B}_{\rm fac}$ varies from one process to another in this class. However, as can be seen from Table II these changes are relatively small (less than 6%). This is caused by the dominance of the part of the amplitude proportional to a_1 over that proportional to a_2. It should be mentioned here that, unlike the other two classes, $\Delta\mathcal{B}_{\rm fac}$ in class III processes is model dependent and the values presented in Table II were calculated based on the BSW II model, to be introduced later in this paper. However, be-

TABLE II. $\Delta\mathcal{B}_{\rm fac}$ represents the percentage change in the branching ratio, assuming factorization, due to NLL values of the Wilson coefficients (column 4) and due to penguin diagrams (column 5). The last column represents the total change.

Processes	Class	Model	$\Delta\mathcal{B}_{\rm fac}$: change in branching ratio		
			NLL effect	Penguin effect	Total change
Type $b\to c\bar{u}d$					
$\bar{B}^0\to D^+\pi^-,\ldots$, etc.	I		0.8%		0.8%
$\bar{B}^0\to D^0\pi^0,\ldots$, etc.	II		−56.7%		−56.7%
$B^-\to D^0\pi^-$	III	BSW II	−4.4%		−4.4%
$B^-\to D^0\rho^-$	III	BSW II	−2.1%		−2.1%
$B^-\to D^0a_1^-$	III	BSW II	−1.1%		−1.1%
$B^-\to D^{*0}\pi^-$	III	BSW II	−6.0%		−6.0%
$B^-\to D^{*0}\rho^-$	III	BSW II	−3.3%		−3.3%
$B^-\to D^{*0}a_1^-$	III	BSW II	−1.8%		−1.8%
Type $b\to c\bar{c}s$					
$B\to DD_s$	I		0.8%	−27%	−26.2%
$B\to DD_s^*$	I		0.8%	−36.0%	−35.2%
$B\to D^*D_s$	I		0.8%	6.4%	7.2%
$B\to D^*D_s^*$	I	BSW II	0.8%	15.1%	15.9%
$B\to KJ/\psi,\ldots$, etc.	II		−56.7%	0.2%	−56.5%
Type $b\to c\bar{c}d$					
$B\to DD^-$	I		0.8%	−23%	−22.2%
$B\to DD^{*-}$	I		0.8%	−25.7%	−24.9%
$B\to D^*D^-$	I		0.8%	5.9%	6.7%
$B\to D^*D^{*-}$	I	BSW II	0.8%	12.9%	13.7%
$B\to\pi J/\psi,\ldots$, etc.	II		−56.7%	0.4%	−56.3%

cause of the dominance of one part of the decay amplitude over the other, this model dependence is not very strong.

Decays of type $b\to c\bar{c}s$ receive contributions from both tree and penguin diagrams and the relevant effective Hamiltonian is given by Eq. (3). In order to extract the factorizable contributions to these processes, an appropriate transformation is needed for the operators Q_5 and Q_6 containing right-handed currents. Using the Fierz transformation, color algebra, and Dirac equation, the decay amplitudes for processes of this type can be easily worked out. For example, assuming naive factorization, symbolized by the subscript ''fac,'' the decay amplitudes for the processes $\bar{B}^0\to D^+D_s^-$ and $\bar{B}^0\to\bar{K}^0J/\psi$ are given by

$$\mathcal{A}_{\rm fac}(\bar{B}^0\to D^+D_s^-)=\frac{G_F}{\sqrt{2}}\left[V_{cb}V_{cs}^*a_1+\sum_{q=u,c}V_{qb}V_{qs}^*\times\left(a_4^q+2a_6^q\frac{m_{D_s}^2}{(m_b-m_c)(m_c+m_s)}\right)\right]\times\langle D^+|(\bar{c}b)_L|\bar{B}^0\rangle\langle D_s^-|(\bar{s}c)_L|0\rangle \quad (7)$$

and

$$\mathcal{A}_{\rm fac}(\bar{B}^0\to\bar{K}^0J/\psi)=\frac{G_F}{\sqrt{2}}\left[V_{cb}V_{cs}^*a_2+\sum_{q=u,c}V_{qb}V_{qs}^*(a_3^q+a_5^q)\right]\times\langle\bar{K}^0|(\bar{s}b)_L|\bar{B}^0\rangle\langle J/\psi|(\bar{c}c)_L|0\rangle, \quad (8)$$

respectively, where

$$a_3^q=C_3^q+\frac{1}{3}C_4^q,\quad a_4^q=C_4^q+\frac{1}{3}C_3^q,$$

$$a_5^q=C_5^q+\frac{1}{3}C_6^q,\quad a_6^q=C_6^q+\frac{1}{3}C_5^q,\quad q=u,c. \quad (9)$$

Note that $N_c=3$ is used for the penguin amplitudes also. If the penguin-generated terms were omitted, the effect of working in NLL order instead of LL order would be very small. In fact, $\Delta\mathcal{B}_{\rm fac}$ is less than 1%, the same as that calculated above for the color-favored decays of type $b\to c\bar{u}d$. However, if the contributions from the penguin diagrams are considered, we get relatively large effects. The branching ratios for the processes $B\to D^+D_s^-$ and $B\to D^+D_s^{*-}$ get reduced by 27% and 36%, respectively, while the branching ratios for $B\to D^*D_s$ and $B\to D^*D_s^*$ are increased by 6% and 15%, respectively (see Table II). To demonstrate the cause of these large changes, let us consider the decay $B\to D^+D_s^-$. In a rough calculation, we substitute the following approximations in Eq. (7): $a_1\approx1$, $a_4^c\approx-0.04$, $a_6^c\approx-0.05$, $V_{ub}V_{us}^*\approx0$, and $m_{D_s}^2/(m_b-m_c)(m_c+m_s)\approx1$. The change in the amplitude due to penguin diagrams is then about $(1-0.04-2\times0.05)^2-1\approx-27\%$. In the case of class II processes, the branching ratios calculated in NLL order are 57% lower than those calculated in LL order (similar to class II processes of type $b\to c\bar{u}d$). The penguin effects, however, turn out to be very small (about 0.2%). This is because the values for a_3 and a_5 are very close in magnitude and have opposite signs, resulting in a mutual cancellation.

The effective Hamiltonian for processes of type $b\to c\bar{c}d$ is similar to Eq. (3) except that the s flavor is replaced by the d flavor. The numerical values for $C_{i=1,\ldots,6}^{\rm eff}$ turn out to be the same as those in Table I without noticeable changes. The decay amplitudes for the processes $B\to DD^-$ (for example) can be written from Eq. (7) by replacing the s flavor by the d flavor. By doing a similar replacement, the amplitude for the process $B\to\pi J/\psi$ can be written from Eq. (8). In Table II, we show the NLL and penguin effects on the calculated branching ratios of these two sets of processes.

IV. ESTIMATION OF THE NONFACTORIZATION PARAMETERS

In Ref. [14], nonfactorization was parametrized through ε_1 and ε_8. These two parameters represent the size of the color-singlet and color-octet nonfactorizable diagrams relative to the factorizable one. By assuming universality (process independence) of these two parameters, we estimated their values in Ref. [15] for Cabibbo-favored B decays. The estimate was done using the available experimental branching ratios for two sets of class I processes ($\bar{B}^0\to D^+\pi^-,D^+\rho^-,D^+a_1^-,D^{*+}\pi^-,D^{*+}\rho^-,D^{*+}a_1^-$ and $B\to DD_s,DD_s^*,D^*D_s,D^*D_s^*$) and one set of class II processes ($B\to KJ/\psi,K\psi(2S),K^*J/\psi,K^*\psi(2S)$). For the Wilson coefficients we [15] used the values calculated up to LL order and neglected all contributions from the penguin diagrams. Regarding the form factors, we used the predictions of the BSW II model. In general, the estimated values of ε_1 and ε_8 improved the agreement with experimental measurements when the notion of factorization was extended to include other channels of B and B_s decays. This supported the assumption of the universality of these parameters in Cabibbo-favored B decays.

According to Eq. (1), nonfactorization contributes to the decay amplitudes of class I and class II processes through the multiplicative factors (omitting the penguin contributions for simplicity of argument)

$$\xi_1=\left(1+\varepsilon_1+\frac{C_2}{a_1}\varepsilon_8\right)\approx\left(1+\varepsilon_1-\frac{1}{3}\varepsilon_8\right) \quad (10)$$

and

$$\xi_2=\left(1+\varepsilon_1+\frac{C_1}{a_2}\varepsilon_8\right)\approx(1+\varepsilon_1+20\varepsilon_8), \quad (11)$$

respectively. The difference between these two factors is in the coefficient of the color-octet parameter. Consequently, in the case of class II processes the long-distance effects in ε_8 are greatly enhanced by the short-distance effects arising

from C_1/a_2. This is in addition to the enhancement of ε_8 over ε_1, by a factor of N_c, according to the rules of QCD. As a result, it may be harmless to ignore the contribution due to the color-singlet parameter ε_1. On the other hand, in class I processes we notice that ε_8 is suppressed by approximately a factor of 1/3 due to short-distance effects. Since this compensates for the enhancement due to QCD, it is not justified to omit ε_1 in this class and the two parameters should be treated on equal footing. From the preceding discussion we infer that class II processes are sensitive probes of ε_8, whereas ε_1 is mainly determined by class I processes, albeit with less sensitivity.

In this work, we reestimate the values of the nonfactorization parameters ε_1 and ε_8 using a χ^2 fit to the experimental branching ratios of the three sets of processes mentioned above. However, for the Wilson coefficients we use the values calculated up to NLL order and include, in the color-singlet part of the amplitude, the contributions from the penguin diagrams. As for the color-octet part, we include the contributions from the operators Q_1 and Q_2 only. For example, the decay amplitude for the process $B\to KJ/\psi$, after including the nonfactorizable contributions, will read

$$\mathcal{A}(B\to KJ/\psi)=\frac{G_F}{\sqrt{2}}V_{cb}V_{cs}^*\Bigg[\Bigg(a_2+\sum_{q=u,c}\frac{V_{qb}V_{qs}^*}{V_{cb}V_{cs}^*}(a_3^q+a_5^q)\Bigg)\times(1+\varepsilon_1)+C_1\varepsilon_8\Bigg]\langle K|(\bar{s}b)_L|B\rangle\times\langle J/\psi|(\bar{c}c)_L|0\rangle. \tag{12}$$

Since the nonfactorization parameters are model dependent, we repeat the χ^2 fit using five different models for the form factors. The first of these models is the original Bauer-Stech-Wirbel model [7] (called BSW I here) where the form factors are calculated at zero-momentum transfer and extrapolated using a monopole form for all the form factors. The second model (called BSW II here) differs from the first one by using a dipole form to extrapolate the form factors F_1, A_0, A_2, and V. This is motivated by the consistency relations in the infinite quark mass limit derived in Ref. [23]. In the third model [23] (called NRSX here) we use the heavy-quark effective theory predictions for the heavy-to-heavy form factors. For the heavy-to-light form factors we use the same values as those predicted by BSW II model. In the fourth model, developed by Altomari and Wolfenstein (AW) [24], the form factors are evaluated at the zero-recoil point corresponding to the maximum momentum transfer and then extrapolated down to the required momentum using a monopole form. In the last model, by Isgur, Scora, Grinstein and Wise (ISGW) [25], the form factors are calculated at the maximum momentum transfer and extrapolated down with an exponential form.

Working, for example, in BSW II model we show in Fig. 1(a) a contour plot of χ^2 in ε_1-ε_8 space. The four minima, labeled 1, 2, 3, and 4, which appear in this figure are to be compared with the corresponding regions in Fig. 2 of Ref.

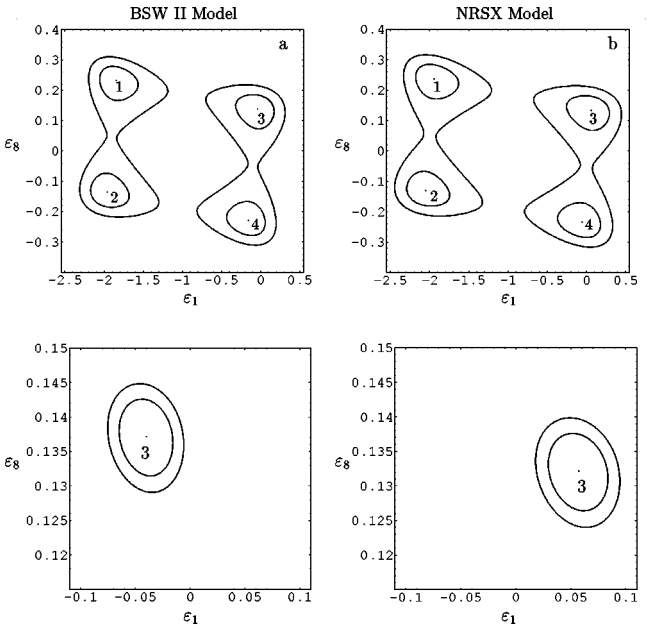

FIG. 1. (a) A contour plot of χ^2 in ε_1-ε_8 space using the BSW II model. (b) A contour plot of χ^2 in ε_1-ε_8 space using the NRSX model. The lower graphs show a magnification of the region containing a minimum of region 3 of χ^2 in the corresponding graphs. The inner closed curve represents a change of $\Delta\chi^2=1$ from the minimum while the outer closed curve represents a change of $\Delta\chi^2=2$.

[15]. The value of χ^2 per degree of freedom (χ^2/d) for these minima is 0.6. In an argument similar to that used in Ref. [15], we exclude solutions 1 and 2 due to the severe violation of the approximate relation $\varepsilon_1/\varepsilon_8=\pm 1/N_c$ suggested by $1/N_c$ expansion. Also, solution 4 is excluded because it produces a negative value for the effective a_2 parameter. So we end up with the estimates $\varepsilon_1=-0.040\pm 0.024$ and $\varepsilon_8=0.137\pm 0.006$. The uncertainties correspond to $\Delta\chi^2=1$. The predictions of the other models are shown in Table III.

Out of the five models considered we note that three (BSW I, ISGW, and AW) do not produce a good fit to the experimental data. This is indicated by the high values of χ^2/d. The remaining two models, on the other hand, produce a good fit to the data with χ^2/d equal to 0.6 for the BSW II model and 0.4 for the NRSX model. In these two models,

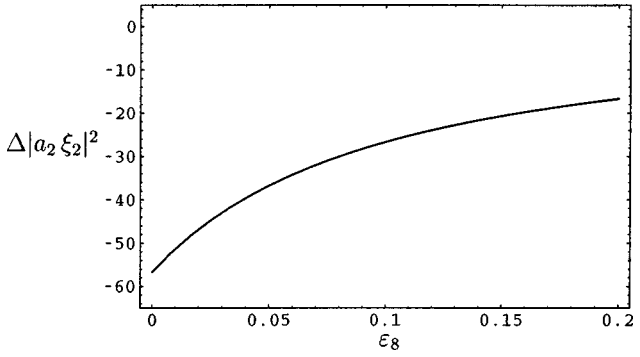

FIG. 2. The percentage difference between $|a_2\xi_2|^2_{LL}$ and $|a_2\xi_2|^2_{NLL}$ as a function of ε_8, taking $\varepsilon_1=0$.

TABLE III. The second and third columns show the estimated nonfactorization parameters ε_1 and ε_8 in different models. The fourth column shows the value of χ^2 per degree of freedom which indicates the goodness of fit. The last two columns show the values of $a_1\xi_1$ and $a_2\xi_2$.

Model	ε_1	ε_8	χ^2/d	$a_1\xi_1$	$a_2\xi_2$
BSW I [7]	-0.037 ± 0.024	0.139 ± 0.006	5.8	0.953	0.216
BSW II [7,28]	-0.040 ± 0.024	0.137 ± 0.006	0.6	0.950	0.213
NRSX [23]	0.057 ± 0.027	0.132 ± 0.006	0.4	1.052	0.213
AW [24]	-0.250 ± 0.019	0.171 ± 0.007	5.7	0.722	0.240
ISGW [25]	-0.071 ± 0.024	0.230 ± 0.008	2.3	0.888	0.318

which show interesting fits, the heavy-to-light form factors are calculated in the same way. So the set of class II processes ($B\to KJ/\psi, \ldots,$ etc.) has the same values for the form factors. This is reflected in the close predictions of ε_8 by both models, which is not the case for the other parameter where the two sets of class I processes take different values for the form factors in the two models. Another point to be noticed is that the NRSX model predicts a destructive interference between the color-singlet and color-octet nonfactorization contributions, causing almost a complete cancellation between the two for class I processes. This is not the case for the other models, which suggest a constructive interference.

V. PREDICTED DECAY RATES INCLUDING NONFACTORIZABLE CONTRIBUTIONS

Using the values estimated for the nonfactorization parameters in a scheme with NLL Wilson coefficients and penguin contributions, we can calculate the branching ratios, in the BSW II model, for all processes considered in the previous work [15]. However, from Table III, we see that the values of $|a_1\xi_1|^2$ and $|a_2\xi_2|^2$ estimated here using the BSW II model do not deviate much from the corresponding values estimated previously in Ref. [15]. Actually, the change in $|a_1\xi_1|^2$ is about 3% and in $|a_2\xi_2|^2$ is about 6%. As a result no significant changes are expected in the branching ratio predictions. An exception is the set of processes ($B\to DD_s, DD_s^*, D^*D_s, D^*D_s^*$) which receive sizable contributions from the penguin diagrams (see Table IV).

By assuming that the universality of ε_1 and ε_8 extends to Cabibbo-suppressed processes, we evaluate the branching ratios for a set of class I processes of type $b\to c\bar{c}d$ and for another set of class II processes of the same type. The results are shown in Table V. These two sets were not considered in the previous work. Our predictions show good agreement with available experimental data which includes the recently measured decay channels $\bar{B}^0\to D^{*+}D^{*-}$ [26] and $B^-\to\pi^- J/\psi$ [27]. In the calculations, the two states $|\eta\rangle$ and $|\eta'\rangle$ are treated in the same way as in [16] where the mixing angle and wave function normalizations are properly taken care of. As for the decay constants we used the values adopted in Ref. [15].

VI. DISCUSSION AND CONCLUSION

In Ref. [15], we demonstrated that naive factorization, in LL order and using tree diagrams only, gives reasonable predictions in comparison with experimental measurements for the branching ratios of class I and class III processes. However, for class II processes the predicted branching ratios were very low. Also, it was demonstrated that including nonfactorizable contributions through the parameters ε_1 and ε_8 improves considerably the predicted branching ratios for the latter class while preserving reasonable predictions for the other two.

In this work, we find that by working in NLL order (with no penguin diagrams) the predicted branching ratios (in naive factorization) of class I and class III processes are very close to the LL predictions and to the experimental values (see Table II). For class II processes, on the other hand, the predicted branching ratios are considerably lower (by about 57%) than the LL predictions, making the disagreement with the experimental values even worse. However, this problem is greatly remedied by including nonfactorizable contribu-

TABLE IV. The branching ratios predicted for a set of Cabibbo-favored B decays in the BSW II model. The values in the second column were calculated by taking $\varepsilon_1(\mu_0)=\varepsilon_8(\mu_0)=0$ whereas the values in the third column were calculated by taking $\varepsilon_1(\mu_0)=-0.040\pm0.024$ and $\varepsilon_8(\mu_0)=0.137\pm0.006$. The last column represents the available experimental measurements.

Process	Fac.	Nonfac.	Expt. [27]
		Branching ratio $\times10^{-3}$	
$B\to DD_s$	10.3 ± 2.2	8.5 ± 1.9	9.8 ± 2.4
$B\to DD_s^*$	7.9 ± 1.6	6.5 ± 1.4	9.4 ± 3.1
$B\to D^*D_s$	8.4 ± 1.8	7.1 ± 1.6	10.4 ± 2.8
$B\to D^*D_s^*$	29.4 ± 5.9	24.9 ± 5.2	22.3 ± 5.7

TABLE V. The branching ratios predicted for a number of Cabibbo-suppressed B decays in the BSW II model. The values in the second column were calculated by taking $\varepsilon_1(\mu_0)=\varepsilon_8(\mu_0)=0$ whereas the values in the third column were calculated by taking $\varepsilon_1(\mu_0)=-0.040\pm0.024$ and $\varepsilon_8(\mu_0)=0.137\pm0.006$. The last column represents the available experimental measurements.

Process	Fac.	Nonfac.	Expt.
		Branching ratio $\times 10^{-4}$	
$\bar{B}^0\to D^+D^-$	3.6 ± 0.7	3.0 ± 0.6	
$\bar{B}^0\to D^+D^{*-}$	3.5 ± 0.7	2.9 ± 0.6	
$\bar{B}^0\to D^{*+}D^-$	2.7 ± 0.6	2.4 ± 0.5	
$\bar{B}^0\to D^{*+}D^{*-}$	9.9 ± 2.0	8.3 ± 1.7	6.2 ± 3.6 [26]
		Branching ratio $\times 10^{-5}$	
$B^-\to\pi^- J/\psi$	0.35 ± 0.03	4.6 ± 0.5	5.0 ± 1.5 [27]
$B^-\to\rho^- J/\psi$	0.51 ± 0.04	6.7 ± 0.7	<77
$B^-\to a_1^- J/\psi$	0.23 ± 0.02	3.0 ± 0.3	<120
$B^-\to\pi^-\psi(2S)$	0.21 ± 0.02	2.8 ± 0.3	
$B^-\to\rho^-\psi(2S)$	0.33 ± 0.03	4.4 ± 0.5	
$B^-\to a_1^-\psi(2S)$	0.11 ± 0.01	1.5 ± 0.2	

tions. Beside the enhancement of the branching ratios of class II processes, the inclusion of nonfactorizable contributions reduces the sensitivity to whether LL or NLL Wilson coefficients are used in the calculation. This is demonstrated in Fig. 2 by plotting the percentage difference between $|a_2\xi_2|^2_{LL}$ and $|a_2\xi_2|^2_{NLL}$ as a function of ε_8, taking $\varepsilon_1=0$. From the graph we see that a 10% contribution to ε_8 reduces the difference between the branching ratios predicted by LL and NLL order to about half that in naive factorization.

Penguin diagrams contribute to processes of types $b\to c\bar{c}s$ and $b\to c\bar{c}d$. In both types, class II processes are affected only slightly by the penguin contributions. This is due to the destructive interference between the different terms, in the amplitude, generated by the penguin diagrams. On the other hand, for class I processes of type $b\to c\bar{c}s$ this cancellation does not happen and the decay amplitudes receive a significant contribution from the penguin diagrams (see Table II). As can be seen from Table III the best fit to the experimental data is produced by the heavy-quark effective theory (contained in the NRSX model), and lends support to the assumption of the universality of the nonfactorizable contributions in B decays.

ACKNOWLEDGMENT

This research was supported by a grant to A.N.K. from the Natural Sciences and Engineering Research Council of Canada.

[1] F.J. Gilman and M.B. Wise, Phys. Rev. D **20**, 2392 (1979).
[2] W.A. Ponce, Phys. Rev. D **23**, 1134 (1981).
[3] R. Rückl, Habilitationsschrift, University of Munich, 1983.
[4] A.J. Buras and P.H. Weisz, Nucl. Phys. **B333**, 66 (1990).
[5] A.J. Buras, M. Jamin, M.E. Lautenbacher, and P.H. Weisz, Nucl. Phys. **B370**, 69 (1992).
[6] G. Buchalla, A. Buras, and M. Lautenbacher, Rev. Mod. Phys. **68**, 1125 (1996).
[7] M. Wirbel, B. Stech, and M. Bauer, Z. Phys. C **29**, 637 (1985); M. Bauer, B. Stech, and M. Wirbel, *ibid.* **34**, 103 (1987).
[8] A. Ali and C. Greub, Phys. Rev. D **57**, 2996 (1998).
[9] A. Ali, G. Kramer, and C.D. Lu, Phys. Rev. D **58**, 094 009 (1998).
[10] H. Cheng and B. Tseng, Phys. Rev. D **58**, 094 005 (1998).
[11] H.Y. Cheng, Phys. Lett. B **335**, 428 (1994); Z. Phys. C **69**, 647 (1996); Phys. Lett. B **395**, 345 (1997).
[12] A. N. Kamal and A. B. Santra, Alberta Report No. Thy 31-94, 1994; Z. Phys. C **72**, 91 (1996).
[13] J. Soares, Phys. Rev. D **51**, 3518 (1995).
[14] M. Neubert and B. Stech, in *Heavy Flavours*, 2nd ed., by A. J. Buras and M. Lindner (World Scientific, Singapore, in press), Report No. CERN-TH/97/99, hep-ph/9705292.
[15] F.M. Al-Shamali and A.N. Kamal, Phys. Rev. D **59**, 054 020 (1999).
[16] F.M. Al-Shamali and A.N. Kamal, Eur. Phys. J. C **4**, 669 (1998).
[17] CLEO Collaboration, C.P. Jessop *et al.*, Phys. Rev. Lett. **79**, 4533 (1997).
[18] R. Fleischer, Z. Phys. C **58**, 483 (1993); **62**, 81 (1994).
[19] G. Kramer, W.F. Palmer, and H. Simma, Nucl. Phys. **B428**, 77 (1994).
[20] A.N. Kamal and C.W. Luo, Phys. Lett. B **393**, 151 (1997).
[21] H. Fusaoka and Y. Koshio, Phys. Rev. D **57**, 3986 (1998).
[22] A. Ali and D. London, Nucl. Phys. B (Proc. Suppl.) **54A**, 297 (1997).
[23] M Neubert, V. Rieckert, B. Stech, and Q. P. Xu, in *Heavy Flavours*, 1st ed., edited by A. J. Buras and M. Lindner (World Scientific, Singapore, 1992), p. 286.

[24] T. Altomari and L. Wolfenstein, Phys. Rev. D **37**, 681 (1988).
[25] N. Isgur, D. Scora, B. Grinstein, and M.B. Wise, Phys. Rev. D **39**, 799 (1989); D. Scora and N. Isgur, *ibid.* **40**, 1491 (1989).
[26] CLEO Collaboration, J.L. Rodriguez, Report No. uh-511-920-98, hep-ex/9901008.
[27] Particle Data Group, C. Caso *et al.*, Eur. Phys. J. C **3**, 1 (1998).
[28] M. Neubert and V. Rieckert, Nucl. Phys. **B382**, 97 (1992).